Effect of Groove Size on Aerodynamic Performance of a Low Reynolds Number UAV Propeller (Part II)

Aravind SEENI*

*Corresponding author
Department of Aeronautical Engineering, Rajalakshmi Engineering College,
Thandalam, Chennai 602 105, India,
aravindseeni.s@rajalakshmi.edu.in

DOI: 10.13111/2066-8201.2022.14.4.11

Received: 07 July 2022/ Accepted: 15 November 2022/ Published: December 2022

Abstract: *Following on from the author's previous work on grooved propellers, numerical investigations are carried out on Applied Precision Composites Slow Flyer 10×7 propeller. Computational Fluid Dynamics is used to analyze the novel design. The grooved sections considered have a rectangular geometry measuring 0.1×0.3mm, 0.2×0.1mm, 0.2×0.2mm and 0.2×0.3mm which are placed at 0.09c, 0.17c, 0.32c and 0.42c from the leading edge. The results of the study showed that the presence of grooves modified the flow characteristics having only a negative impact on the thrust performance. However, the grooves improved the power performance due to torque reduction. The analysis of the K_P results showed, in most models, the low torque relative to the baseline in the operational range of the low to medium advance ratio range. However, the improvement in torque did not improve the efficiency in all models.*

Key Words: *passive flow control, grooved propeller, aerodynamic performance, UAV range, UAV endurance*

1. INTRODUCTION

The research described in this paper is an extension of the earlier work by the same author entitled "Effect of Groove Size on Aerodynamic Performance of a Low Reynolds Number UAV Propeller" published *in INCAS Bulletin, Vol. 14, Issue 1, pp. 171-186, 2022* [1].

In the earlier published research, 7 models namely, Model − 1 to Model − 7 are analysed and the performance and efficiency results reported. In this paper, the focus is on the results obtained for 10 additional models.

Research on improving the efficiency of UAV propellers helps to increase and add value to future applications of drones. The desired design requirement is a propelling device capable of producing improved thrust and reduced torque at a low Re. Modern research is concerned with improving the thrust through flow modifiers or flow control technique. These flow modifiers alter the fluid flow such that the flow trajectory is optimized around the aerodynamic body to attain the desired performance.

The current research is concerned with studying the flow control technique called grooved design. In the present study, a comprehensive study on grooved propeller design has been performed with the aim to study its significance for the aeronautical application. The unique features of an aeronautical propeller are low torque, high thrust and high efficiency during

operation. The effect of the variation in groove size on the performance characteristics of the propeller will be investigated. The size variation of grooves could have either favorable or detrimental impact on the aerodynamic performance. These have not been investigated so far and will be investigated in the current work.

2. METHODOLOGY

As in the earlier paper, CFD is used to solve the governing equations of the fluid flow. RANS simulations are performed with different propeller models as a first step of initiating the research on fluid dynamic analysis of grooved propeller.

2.1 Baseline propeller

Applied Precision Composites (APC) 10×7 *Slow Flyer (SF)* is considered as the baseline propeller in this study. APC10x7SF is widely used in low *Re* applications such as small-scale UAVs. This propeller is chosen based on the availability of data from the experiments of Brandt *et al.* [2]. The propeller has a diameter (D) of 0.254 m and a pitch of 0.1778 m. Low *Re* Eppler E63 airfoil sections near the hub and thin Clark-Y airfoil sections near the tip are used to design the propeller. For the simulation, the propeller is assumed to be rotating at a constant rotational speed of 3008 rpm.

2.2 CAD modelling

The design of propellers is performed using CAD software Catia v5. For the design of grooved propeller, the baseline propeller model is modified with grooves of varying dimensions. To study the effect of groove geometry, grooves are placed at specific positions from the leading edge at 0.09c, 0.17c,0.32c and 0.42c distance. The dimensions of the grooves are varied for different positions, as listed in Table 1.

Table 1 – Propeller configurations to study the effect of groove geometry

Name	Groove size, mm	Groove position, x_{LE}
Model − 8	0.1mm × 0.3mm	0.09c
Model − 9	0.1mm × 0.3mm	0.17c
Model − 10	0.1mm × 0.3mm	0.32c
Model − 11	0.1mm × 0.3mm	0.42c
Model − 12	0.2mm × 0.1mm	0.09c
Model − 13	0.2mm × 0.1mm	0.17c
Model − 14	0.2mm × 0.2mm	0.17c
Model − 15	0.2mm × 0.2mm	0.32c
Model − 16	0.2mm × 0.3mm	0.17c
Model − 17	0.2mm × 0.3mm	0.32c

2.3. Computational Fluid Dynamics

2.3.1 Computational domain

The computational domain consists of a 3D computational grid. A Multiple Reference Frame (MRF) approach is implemented to model the computational domain. Two reference frames comprising a stationary and a rotational frame are assumed. The propeller is enclosed within the rotational reference frame which rotates at a speed of 3008 rpm. The rotational reference

frame is designed with a cylindrical geometry having a diameter of 1.1D. The stationary reference frame is a cubic enclosure and designed with a constant side length of 8D.

2.3.2 Mesh

The domain is meshed into multiple numbers of small fluid control volumes in which the velocity components u, v and w and pressure component p at the centre of all the control volumes are solved. An unstructured mesh consisting of tetrahedron elements is used. The mesh for the grooved designs is performed with identical grid sizes of the baseline propeller. The meshes in the groove locations are maintained at sufficient mesh density in order to accurately capture the flow characteristics.

2.3.3 Boundary conditions and settings

At the wall, which is the rotating domain, a no slip condition is assumed. Inlet fluid velocities ranging between 2.4384 m/s and 10.1473 m/s for corresponding J conditions between 0.192 and 0.799 are assumed. For pressure-velocity coupling, Semi-Implicit Method for Pressure-Linked Equations (SIMPLE) scheme is assumed. The gradients are assigned with Least-Squares Cell-based algorithm. The standard scheme of interpolation is assigned for pressure. For Turbulent Dissipation Rate, Turbulent Kinetic Energy and momentum, a second order upwind interpolation scheme is applied. The fluid is assumed to be air with the following properties: T=25ºC, ρ=1.225 kg/m^3 and μ=1.7894×10^{-5} kgm^{-1}s^{-1}. The flow is assumed to be steady, viscous and incompressible. The one-equation Spalart-Allmaras (S-A) model will provide turbulence closure. The S-A model is selected based on its application in aerodynamic flows.

2.4 Expressions for aerodynamic coefficients of a propeller

The coefficients representing the aerodynamic performance of propeller are provided. The thrust coefficient can be expressed as in Eqn. 1.

$$K_T = \frac{T}{\rho n^2 D^4} \tag{1}$$

where T is the thrust force, ρ is the fluid density, n is the rotational speed, and D is the diameter. The torque coefficient can be expressed as in Eqn. 2.

$$K_Q = \frac{Q}{\rho n^2 D^5} \tag{2}$$

where Q is the torque. The power coefficient can be expressed as in Eqn. 3.

$$K_P = \frac{P}{\rho n^3 D^5} \tag{3}$$

where P is power. P is estimated from torque Q and propeller speed as in Eqn. 4:

$$P = 2\pi n Q \tag{4}$$

The efficiency is a function of K_T, K_P and J and can be expressed as in Eqn. 5. Also, it can be expressed as per Eqn. 6.

$$\eta = J\frac{K_T}{K_P} \tag{5}$$

$$\eta = \frac{J}{2\pi}\frac{K_T}{K_Q} \tag{6}$$

For the propeller case, the errors are estimated again by comparing CFD obtained numerical results with experimental data. The percentage difference in error for various performance coefficients between numerical and experimental results will be estimated using the expressions as given in Eqns. 7-9.

$$\Delta K_T(\%) = \frac{K_{T,CFD} - K_{T,EXP}}{K_{T,EXP}} \times 100 \tag{7}$$

$$\Delta K_P(\%) = \frac{K_{P,CFD} - K_{P,EXP}}{K_{P,EXP}} \times 100 \tag{8}$$

$$\Delta \eta(\%) = \frac{\eta_{CFD} - \eta_{EXP}}{\eta_{EXP}} \times 100 \tag{9}$$

where $K_{T,EXP}$ refers to experimental K_T of baseline design, $K_{T,CFD}$ refers to numerical K_T of grooved design, $K_{P,EXP}$ refers to experimental K_P of baseline design, $K_{P,EXP}$ refers to numerical K_P of grooved design, η_{EXP} refers to experimental η of baseline design, η_{FD} refers to numerical η of grooved design.

3. RESULTS AND DISCUSSIONS

3.1 Verification and validation

The verification and validation of the model for the baseline propeller is provided in Seeni [1].

3.2 Effect of groove size on propeller performance

3.2.1 Model − 8

The performance and efficiency results of Model − 8 grooved design are provided in Table 2.

Model − 8 grooved design exhibited underperforming K_T for J between 0.192 to 0.717. The difference lies in the range between −7.67% to −14.62%.

For high J, 0.773 and 0.799 K_T increased relative to the baseline design. K_P decreased for J between 0.192 to 0.659.

From J between 0.717 to 0.799, the K_P increased. η of the grooved design was found to be lower compared to baseline for all J cases.

The three-dimensional velocity distribution of the fluid surrounding the Model−8 grooved propeller is modified or reduced to detrimentally affect thrust.

The velocity distribution along a plane bisecting the flow field along y-z for two J case samples, 0.334 and 0.573 is shown in Fig. 1.

For J=0.334, the peak velocity is decreased at the blade tip. For J=0.573, the peak velocity is maintained constant to J=0.334 although at a slight reduction to baseline. This shows that the results are not affected by the freestream velocity change or J.

The velocity modifications in the presence of the groove modifies the pressure distribution to affect the thrust.

Lower peak pressures are maintained at the pressure side (aft) as compared to baseline whereas higher low pressures are maintained at the suction side (fore) as compared to baseline for both J=0.334 and J=0.573 cases.

Fig. 2 shows the modified pressure levels on the pressure side and on the suction side in the presence of groove for two J cases, 0.334 and 0.573 when viewed along the y-z plane bisecting the flow field.

Table 2 – Performance and efficiency results of Model − 8

Case	Condition J	K_T	ΔK_T [%]	$10K_P$	ΔK_P [%]	η [%]	$\Delta\eta$ [%]
1	0.192	0.1073	−14.62	0.6290	−7.64	32.76	−7.72
2	0.236	0.1036	−12.29	0.6241	−5.72	39.17	−6.96
3	0.282	0.0985	−11.16	0.6136	−5.01	45.28	−6.45
4	0.334	0.0924	−10.05	0.5993	−4.72	51.48	−5.71
5	0.383	0.0859	−9.55	0.5825	−4.51	56.50	−5.20
6	0.432	0.0789	−8.79	0.5623	−4.05	60.62	−5.13
7	0.486	0.0704	−8.05	0.5355	−3.16	63.92	−5.16
8	0.527	0.0634	−8.41	0.5113	−2.79	65.32	−5.87
9	0.573	0.0552	−9.14	0.4814	−2.14	65.64	−7.28
10	0.628	0.0447	−9.30	0.4408	−0.72	63.70	−8.60
11	0.659	0.0386	−9.30	0.4165	−0.11	61.13	−9.30
12	0.717	0.0268	−7.67	0.3664	3.21	52.40	−10.58
13	0.773	0.0147	2.52	0.3146	11.17	36.02	−7.88
14	0.799	0.0089	13.77	0.2877	14.15	24.65	−0.21

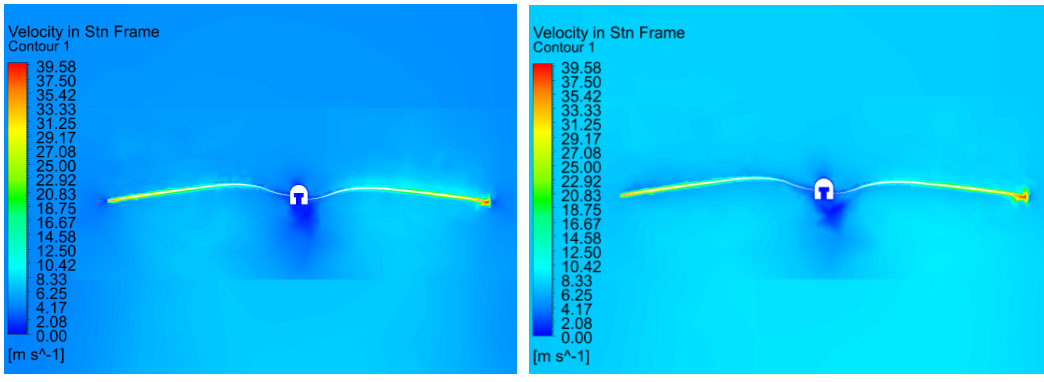

(a) (b)

Fig. 1 – Velocity flow-field around Model − 8 propeller for (a) J=0.334 and (b) J=0.573

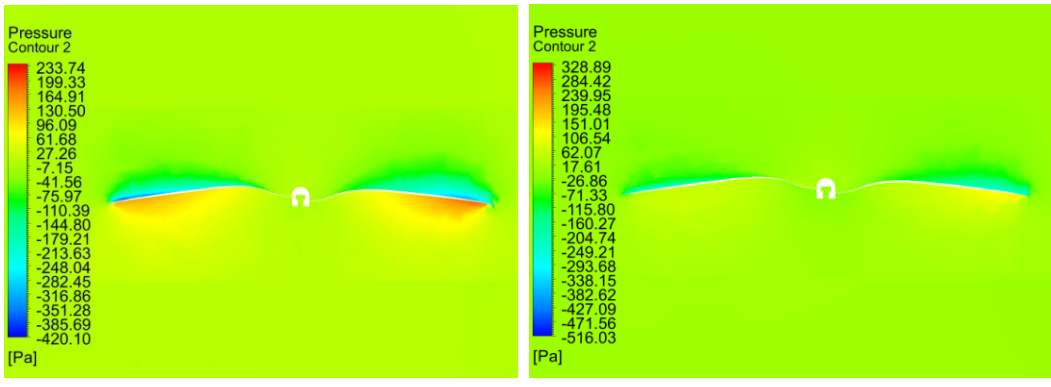

(a) (b)

Fig. 2 – Pressure contour of flow around Model − 8 propeller for (a) J=0.334 and (b) J=0.573

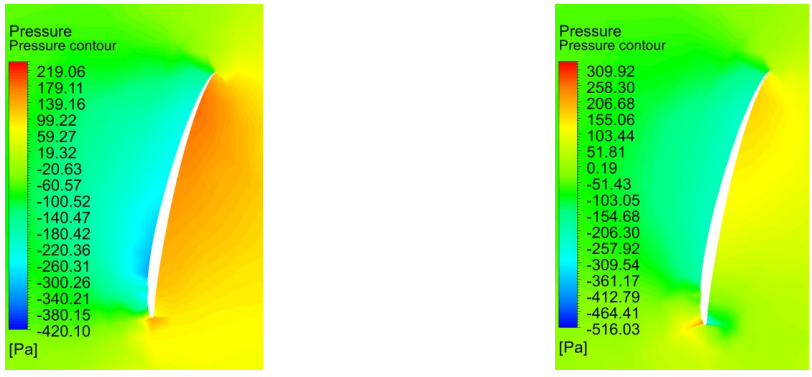

(a) (b)

Fig. 3 – Pressure contour of flow around Model − 8 propeller at 0.75R radial distance for (a) J=0.334 and (b) J=0.573

The presence of the groove, in addition to thrust, also reduces the reactional torque according to Newton's third law. The torque of propeller for Model − 8 grooved design is modified due to the reduction or increment in reactional moment in the presence of the groove. This has resulted in change in K_P. For Model − 8, with increase in J, K_P decreases even more in the presence of groove for J from 0.192 to 0.659 and increases for J from 0.717 to 0.799 which is presented as ΔK_P in Table 2.

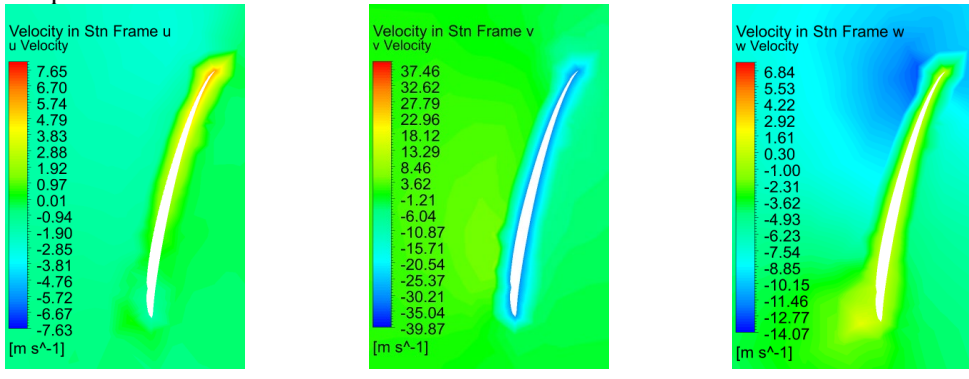

(a) (b) (c)

Fig. 4 – Velocity contour of flow around Model − 8 propeller at 0.75R radial distance for J=0.334 (a) radial component (b) rotational component (c) axial component

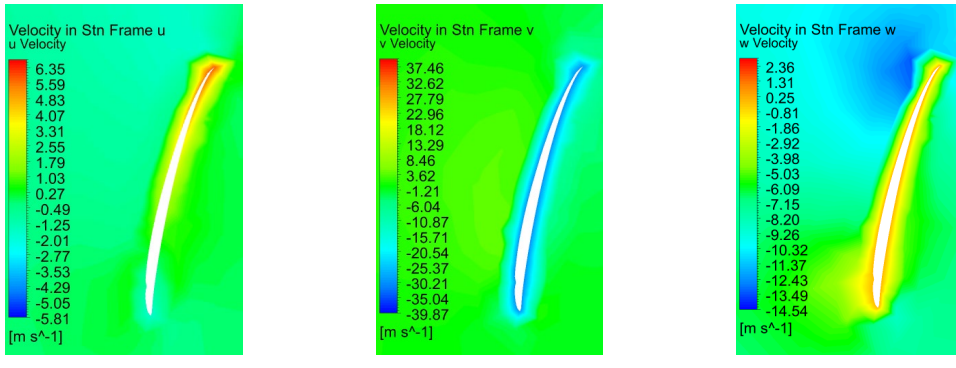

(a) (b) (c)

Fig. 5 – Velocity contour of flow around Model − 8 propeller at 0.75R radial distance for J=0.573 (a) radial component (b) rotational component (c) axial component

The decomposition of velocity in the radial (u- component), rotational (v- component) and axial (w- component) directions are presented in Fig. 4 for J=0.334 and in Fig. 5 for J=0.573. During rotation, the fluid velocity is modified when traversing between leading edge and trailing edge and when traversing the groove.

For J=0.334, the magnitude of the peak radial velocity component is increased, peak rotational velocity component remains close to baseline and peak axial velocity component is reduced compared to baseline. The magnitude of low radial velocity component for this J is increased, low rotational velocity component remains close to baseline and low axial velocity component is increased compared to baseline.

For J=0.573, the magnitude of the peak radial velocity component is increased, peak rotational velocity component remains close to baseline and peak axial velocity component is increased compared to baseline. The magnitude of low radial velocity component for this J is increased, low rotational velocity component remains close to baseline and low axial velocity component is increased compared to baseline. Vector plots of fluid flow at 0.75R radial distance and velocity distribution for three-dimensional Model − 8 propeller is provided in Fig. 6 for single J condition J=0.334 to illustrate that the velocity very near to the blade surface is modified in the presence of groove.

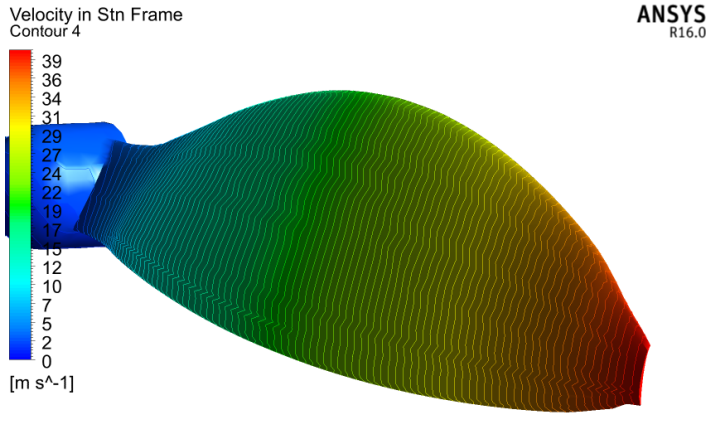

Fig. 6 – Velocity distribution on Model − 8 propeller blade for J=0.334

A measure of turbulence can be provided through TKE which is a turbulence quantity. Model − 8 grooved design has increased TKE along the blade radii compared to baseline for J=0.334 (Fig. 7(a)). For J=0.573, the TKE is decreased (Fig. 7(b)).

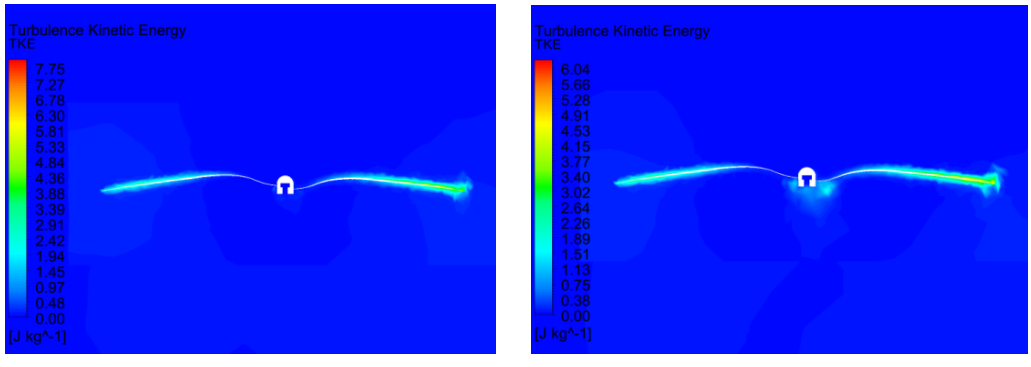

(a) (b)

Fig. 7 – Turbulence Kinetic Energy of Model − 8 propeller for (a) J=0.334 and (b) J=0.573

3.2.2 Model − 9

The performance and efficiency results of Model − 9 grooved design are provided in Table 3. The relative difference between the results with baseline propeller is also listed in the table.

K_T for Model − 9 grooved design showed decreased K_T for 12 cases of J ranging from 0.192 to 0.717.

The decrement was in the range between −7.41% to −14.51%. K_P was found to be reduced for 9 cases of J ranging from 0.192 to 0.573.

From J of 0.628, the K_P increased relative to baseline. The η was found to be reduced for all cases of J except for case 14 with J of 0.799.

Table 3 – Performance and efficiency results of Model − 9

Case	Condition J	K_T	ΔK_T [%]	$10K_P$	ΔK_P [%]	η [%]	$\Delta\eta$ [%]
1	0.192	0.1075	−14.51	0.6340	−6.90	32.54	−8.33
2	0.236	0.1035	−12.36	0.6273	−5.24	38.94	−7.51
3	0.282	0.0987	−10.99	0.6184	−4.28	45.02	−6.99
4	0.334	0.0929	−9.56	0.6045	−3.89	51.32	−6.01
5	0.383	0.0864	−9.07	0.5879	−3.62	56.28	−5.58
6	0.432	0.0794	−8.20	0.5677	−3.12	60.43	−5.43
7	0.486	0.0711	−7.23	0.5410	−2.18	63.84	−5.28
8	0.527	0.0638	−7.75	0.5157	−1.96	65.24	−5.99
9	0.573	0.0559	−7.89	0.4881	−0.80	65.64	−7.29
10	0.628	0.0453	−8.15	0.4466	0.59	63.67	−8.64
11	0.659	0.0390	−8.35	0.4209	0.93	61.13	−9.30
12	0.717	0.0269	−7.41	0.3671	3.41	52.44	−10.50
13	0.773	0.0150	4.72	0.3128	10.53	37.01	−5.36
14	0.799	0.0094	19.97	0.2885	14.49	25.91	4.92

Table 4 – Performance and efficiency results of Model − 10

Case	Condition J	K_T	ΔK_T [%]	$10K_P$	ΔK_P [%]	η [%]	$\Delta\eta$ [%]
1	0.192	0.1079	−14.19	0.6329	−7.06	32.72	−7.82
2	0.236	0.1040	−11.92	0.6259	−5.45	39.22	−6.84
3	0.282	0.0988	−10.91	0.6150	−4.80	45.30	−6.40
4	0.334	0.0927	−9.76	0.6020	−4.29	51.42	−5.83
5	0.383	0.0864	−9.01	0.5869	−3.79	56.41	−5.35
6	0.432	0.0795	−8.04	0.5674	−3.17	60.57	−5.22
7	0.486	0.0710	−7.27	0.5409	−2.18	63.81	−5.32
8	0.527	0.0641	−7.35	0.5176	−1.59	65.27	−5.95
9	0.573	0.0559	−7.85	0.4869	−1.04	65.83	−7.02
10	0.628	0.0454	−7.96	0.4462	0.49	63.87	−8.37
11	0.659	0.0392	−7.94	0.4209	0.93	61.40	−8.90
12	0.717	0.0271	−6.60	0.3707	4.42	52.39	−10.59
13	0.773	0.0150	4.91	0.3172	12.09	36.56	−6.50
14	0.799	0.0095	21.22	0.2903	15.19	26.03	5.37

3.2.3 Model − 10

The performance and efficiency results of Model − 10 grooved design are provided in Table 4. The relative difference between the results with baseline propeller is also listed in the table.

Model−10 grooved design provided K_T underperforming for 12 cases of J in the range from 0.192 to 0.717. K_T varied between − 6.60% to − 14.19% in this range. For higher J of 0.773 and 0.799, K_T improved with respect to baseline by 4.91% and 21.22% respectively. K_P varied between − 1.04% and − 7.06% for J range between 0.192 and 0.573. For J from 0.628, the K_P increased with respect to baseline in the range of 0.49% to 15.19%. η was found to be decreased relative to baseline for all but one case of J. For J between 0.192 to 0.773, and the decrement was in the range of − 5.22% to − 10.59%. For one single case of J 0.799, η was slightly higher than the baseline.

3.2.4 Model − 11

The performance and efficiency results of Model − 11 grooved design are provided in Table 5. The relative difference between the results with baseline propeller is also listed in the table.

Table 5 – Performance and efficiency results of Model − 11

Case	Condition J	K_T	ΔK_T [%]	$10K_P$	ΔK_P [%]	η [%]	$\Delta\eta$ [%]
1	0.192	0.1070	−14.87	0.6302	−7.46	32.60	−8.16
2	0.236	0.1031	−12.74	0.6240	−5.75	38.98	−7.41
3	0.282	0.0980	−11.65	0.6139	−4.97	45.01	−7.01
4	0.334	0.0919	−10.52	0.6001	−4.60	51.15	−6.32
5	0.383	0.0854	−10.08	0.5829	−4.44	56.13	−5.83
6	0.432	0.0782	−9.62	0.5621	−4.08	60.09	−5.97
7	0.486	0.0697	−9.04	0.5345	−3.35	63.35	−6.00
8	0.527	0.0628	−9.20	0.5108	−2.90	64.83	−6.58
9	0.573	0.0544	−10.39	0.4801	−2.42	64.91	−8.31
10	0.628	0.0441	−10.62	0.4391	−1.11	63.02	−9.58
11	0.659	0.0379	−11.12	0.4134	−0.87	60.36	−10.44
12	0.717	0.0264	−9.01	0.3621	2.01	52.24	−10.85
13	0.773	0.0139	−3.01	0.3105	9.72	34.53	−11.70
14	0.799	0.0082	5.19	0.2842	12.79	23.06	−6.62

Model − 11 grooved design produced K_T without any relative increase compared to baseline for 13 cases of J from 0.192 to 0.773. For only one case of J of 0.799, K_T increased by 5.19% relative to baseline. K_P was found to be reduced for 11 cases of J from 0.192 to 0.659. The decrement varied between − 0.87% and − 7.46%. For J between 0.717 and 0.799, the K_P increased relative to baseline. η for this grooved design showed negative improvements compared to baseline. η ranged from − 5.83% to − 11.70% for the 14 J cases considered.

3.2.5 Model − 12

The performance and efficiency results of Model − 12 grooved design are provided in Table 6. The relative difference between the results with baseline propeller is also listed.

Model − 12 grooved design attained “wind-milling” state before developing a negative thrust for the lowest J case of 0.192. At this J, the propeller produced negative thrust. For J from 0.236 to 0.717, K_T was found to be reduced compared to baseline. Only for J of 0.773

and 0.799, K_T was found to be improved relative to the baseline design. K_P was found to be decreased for J from 0.192 to 0.573. At J of 0.628, the K_P was found to be equal to baseline. Beyond this case of J, the K_P was found to be increased relative to baseline. η was found to be decreased for 13 cases of J from 0.192 to 0.773. Due to attaining wind-milling state, η dropped by −100.2% for 0.192 J. Only for one case of J of 0.799, and η was found to be increased.

Table 6 – Performance and efficiency results of Model − 12

Case	Condition J	K_T	ΔK_T [%]	$10K_P$	ΔK_P [%]	η [%]	$\Delta\eta$ [%]
1	0.192	−0.0001	−100.11	0.6297	−7.53	−0.04	−100.12
2	0.236	0.1025	−13.23	0.6248	−5.62	38.71	−8.06
3	0.282	0.0981	−11.50	0.6122	−5.24	45.21	−6.59
4	0.334	0.0915	−10.95	0.5966	−5.15	51.20	−6.23
5	0.383	0.0853	−10.22	0.5810	−4.76	56.22	−5.66
6	0.432	0.0779	−9.91	0.5605	−4.35	60.06	−6.01
7	0.486	0.0700	−8.67	0.5368	−2.93	63.34	−6.03
8	0.527	0.0631	−8.76	0.5131	−2.44	64.85	−6.56
9	0.573	0.0555	−8.64	0.4818	−2.07	65.95	−6.85
10	0.628	0.0447	−9.31	0.4440	0.00	63.24	−9.27
11	0.659	0.0388	−8.99	0.4192	0.52	60.95	−9.57
12	0.717	0.0270	−6.92	0.3692	4.01	52.42	−10.55
13	0.773	0.0152	6.09	0.3136	10.82	37.39	−4.37
14	0.799	0.0091	17.10	0.2868	13.82	25.44	3.01

Table 7 – Performance and efficiency results of Model − 13

Case	Condition J	K_T	ΔK_T [%]	$10K_P$	ΔK_P [%]	η [%]	$\Delta\eta$ [%]
1	0.192	0.1091	−6.36	0.6381	−6.30	32.82	0.81
2	0.236	0.1049	−6.71	0.6307	−4.72	39.26	1.19
3	0.282	0.0985	−8.51	0.6170	−4.49	45.03	0.71
4	0.334	0.0923	−9.05	0.6027	−4.18	51.15	1.12
5	0.383	0.0871	−8.33	0.5884	−3.53	56.66	2.22
6	0.432	0.0804	−8.64	0.5706	−2.62	60.84	2.33
7	0.486	0.0705	−11.09	0.5397	−2.41	63.46	1.02
8	0.527	0.0647	−10.21	0.5174	−1.64	65.92	2.30
9	0.573	0.0568	−10.71	0.4884	−0.74	66.62	1.96
10	0.628	0.0467	−11.41	0.4503	1.42	65.15	1.23
11	0.659	0.0402	−12.51	0.4234	1.54	62.60	0.63
12	0.717	0.0283	−14.38	0.3743	5.44	54.24	−1.95
13	0.773	0.0162	−16.53	0.3211	13.47	39.05	−5.25
14	0.799	0.0103	−20.00	0.2945	16.88	27.85	−9.63

3.2.6 Model − 13

The performance and efficiency results of Model − 13 grooved design are provided in Table 7. The relative difference between the results with baseline propeller is also listed.

K_T for Model − 13 grooved design was found to be decreased for all J cases analysed. The decrement varied between − 6.36% for the lowest J case of 0.192 and − 20.0% for the highest

J. K_P was found to be decreased for 9 cases of *J*. The decrement varied from − 0.74% to − 0.63% for *J* between 0.192 and 0.573.

As *J* increased, from 0.628, the K_P increased. The increment was found to be in the range between 1.42% and16.88%. Despite decrement of thrust, η showed a slight improvement for 11 cases of *J* between 0.192 and 0.659. η increase is in the range between 0.63% and 2.33%. For the rest of the cases of *J*, from 0.717 to 0.799, η decreased.

3.2.7 Model − 14

The performance results of Model − 14 grooved design are provided in Table 8. The relative difference between the results with baseline propeller is also listed.

Table 8 – Performance and efficiency results of Model − 14

Case	Condition *J*	K_T	ΔK_T [%]	$10K_P$	ΔK_P [%]	η [%]	$\Delta\eta$ [%]
1	0.192	0.1010	−19.65	0.6116	−10.19	31.70	−10.69
2	0.236	0.1020	−13.63	0.6186	−6.56	38.92	−7.56
3	0.282	0.0973	−12.24	0.6100	−5.57	44.99	−7.04
4	0.334	0.0913	−11.11	0.5957	−5.29	51.19	−6.25
5	0.383	0.0853	−10.18	0.5830	−4.43	56.06	−5.94
6	0.432	0.0782	−9.60	0.5630	−3.93	60.00	−6.10
7	0.486	0.0698	−8.88	0.5356	−3.14	63.33	−6.04
8	0.527	0.0627	−9.43	0.5103	−2.98	64.73	−6.74
9	0.573	0.0544	−10.42	0.4797	−2.51	64.96	−8.25
10	0.628	0.0439	−11.01	0.4390	−1.13	62.76	−9.95
11	0.659	0.0378	−11.35	0.4124	−1.10	60.34	−10.47
12	0.717	0.0260	−10.46	0.3666	3.27	50.79	−13.33
13	0.773	0.0143	−0.34	0.3136	10.80	35.13	−10.14
14	0.799	0.0079	1.61	0.2865	13.71	22.10	−10.53

K_T for Model − 14 grooved design showed negative improvement for 13 cases of *J* (0.192 to 0.773). The decrement varied between − 0.34% to − 19.65%. For *J* of 0.799, K_T showed a slight improvement compared to baseline.

K_P decreased for *J* from 0.192 to 0.659. From *J* of 0.717 to 0.799, the K_P increased relative to baseline. η was found to be decreased for all *J* cases considered. The decrement varied between − 6.04% and − 13.33%.

3.2.8 Model − 15

The performance and efficiency results of Model − 15 grooved design are provided inTable 9. The relative difference between the results with baseline propeller is also listed in the table.

Model − 15 grooved design provided underperforming K_T for 12 cases of *J*. K_T difference varied in the range of − 8.51% to − 14.62% for *J* from 0.192 to 0.717. For *J* of 0.773 and 0.799, K_T increased relative to baseline at 3.02% and 17.98% respectively.

K_P for the grooved design decreased for 9 cases of *J* from 0.192 to 0.573. From *J* of 0.628, the K_P increased relative to baseline.

For all but one *J* case, the η for this grooved design decreased relative to baseline. η decrement can be found in the range of − 6.06% to − 12.48%. For the last case of *J* 0.799, η showed a marginal increase.

Table 9 – Performance and efficiency results of Model − 15

Case	Condition J	K_T	ΔK_T [%]	$10K_P$	ΔK_P [%]	η [%]	$\Delta\eta$ [%]
1	0.192	0.1073	−14.62	0.6343	−6.86	32.48	−8.49
2	0.236	0.1032	−12.62	0.6273	−5.24	38.83	−7.78
3	0.282	0.0982	−11.45	0.6163	−4.59	44.93	−7.17
4	0.334	0.0920	−10.41	0.6019	−4.31	51.06	−6.48
5	0.383	0.0856	−9.93	0.5859	−3.95	55.93	−6.16
6	0.432	0.0784	−9.35	0.5648	−3.61	59.97	−6.14
7	0.486	0.0699	−8.77	0.5364	−3.00	63.31	−6.06
8	0.527	0.0629	−9.11	0.5117	−2.73	64.78	−6.66
9	0.573	0.0549	−9.52	0.4837	−1.69	65.06	−8.10
10	0.628	0.0444	−9.95	0.4441	0.01	62.79	−9.92
11	0.659	0.0382	−10.30	0.4199	0.70	59.97	−11.03
12	0.717	0.0265	−8.51	0.3709	4.49	51.28	−12.48
13	0.773	0.0147	3.02	0.3201	13.11	35.58	−9.01
14	0.799	0.0092	17.98	0.2966	17.69	24.79	0.37

Table 10 – Performance and efficiency results of Model − 16

Case	Condition J	K_T	ΔK_T [%]	$10K_P$	ΔK_P [%]	η [%]	$\Delta\eta$ [%]
1	0.192	0.1072	−14.74	0.6342	−6.87	32.44	−8.61
2	0.236	0.1025	−13.24	0.6247	−5.63	38.70	−8.07
3	0.282	0.0983	−11.40	0.6193	−4.14	44.74	−7.56
4	0.334	0.0922	−10.19	0.6065	−3.58	50.79	−6.97
5	0.383	0.0858	−9.65	0.5894	−3.38	55.78	−6.41
6	0.432	0.0792	−8.48	0.5697	−2.79	60.03	−6.05
7	0.486	0.0708	−7.61	0.5425	−1.90	63.40	−5.93
8	0.527	0.0638	−7.82	0.5183	−1.46	64.85	−6.55
9	0.573	0.0555	−8.63	0.4866	−1.10	65.31	−7.75
10	0.628	0.0452	−8.28	0.4470	0.69	63.52	−8.87
11	0.659	0.0390	−8.40	0.4213	1.02	61.05	−9.43
12	0.717	0.0277	−4.62	0.3688	3.89	53.78	−8.23
13	0.773	0.0151	5.46	0.3136	10.83	37.17	−4.95
14	0.799	0.0097	23.86	0.2891	14.73	26.70	8.09

3.2.9 Model − 16

The performance and efficiency results of Model−16 grooved design are provided in Table 10. The relative difference between the results with baseline propeller is also listed in the table. K_T for Model−16 grooved design varied in the range of − 4.62% to − 14.74% for J between 0.192 and 0.717.

For higher J of 0.773 and 0.799, K_T showed a relative increase compared to baseline. K_P for this grooved model decreased for J from 0.192 to 0.573.

From J of 0.628, K_P increased relative to baseline. η for all J showed a relative decrement of −4.95% to −9.43% for J from 0.192 to 0.773. For the J 0.799, η was found to be increased.

3.2.10 Model − 17

The performance and efficiency results of Model − 17 grooved design are provided in Table 11. The relative difference between the results with baseline propeller is also listed in the table.

Table 11 – Performance and efficiency results of Model − 17

Case	Condition J	K_T	ΔK_T [%]	$10K_P$	ΔK_P [%]	η [%]	$\Delta\eta$ [%]
1	0.192	0.1066	−15.16	0.6319	−7.22	32.40	−8.72
2	0.236	0.1026	−13.10	0.6256	−5.49	38.71	−8.05
3	0.282	0.0977	−11.94	0.6145	−4.88	44.82	−7.40
4	0.334	0.0918	−10.58	0.6016	−4.35	50.98	−6.63
5	0.383	0.0857	−9.76	0.5878	−3.64	55.86	−6.28
6	0.432	0.0787	−8.96	0.5670	−3.24	60.00	−6.11
7	0.486	0.0702	−8.37	0.5405	−2.26	63.11	−6.36
8	0.527	0.0634	−8.41	0.5168	−1.75	64.63	−6.87
9	0.573	0.0551	−9.20	0.4871	−1.00	64.83	−8.43
10	0.628	0.0448	−9.18	0.4481	0.92	62.76	−9.96
11	0.659	0.0386	−9.50	0.4224	1.29	60.15	−10.76
12	0.717	0.0265	−8.72	0.3701	4.26	51.28	−12.49
13	0.773	0.0147	2.47	0.3191	12.74	35.50	−9.21
14	0.799	0.0095	21.72	0.2950	17.05	25.72	4.11

K_T for Model − 17 grooved design showed a relative decrease of − 8.72% to − 15.16% for J between 0.192 and 0.717. From 0.773 J, K_T increased relative to baseline. K_P for this grooved model showed relative decrement for J between 0.192 and 0.573. For J between 0.628 and 0.799, K_P decreased relative to baseline. η of the grooved design decreased in the range of − 6.11% to − 12.49% for J between 0.192 and 0.773. For one case of J, 0.799, η showed improvement for grooved design relative to the baseline design.

3.3 The implication of results for UAV flight operations

Model − 9, Model − 10, Model − 12, Model − 15, Model − 16 and Model − 17 grooved designs had improved η over baseline only for one J of 0.799. Hence η improvement gained from this design is very limited.

Model − 3, Model − 4, Model − 7, Model − 8, Model − 11 and Model − 14 had no η improvement over baseline for all J.

The range of J that provides η improvement is limited. Model − 13 grooved design showed improved η over baseline for J cases 0.192 to 0.659, hence can be operated in a relatively wide range of J compared to other models. η, however, decreased from J of 0.717, hence at higher V, η is reduced.

4. CONCLUSIONS

Research on grooved design implemented on a UAV propeller has been completed. A CFD investigation is conducted on propellers with different groove sizes. 10 grooved designs with different cross-sections namely, 0.1 × 0.3 mm, 0.2 × 0.1 mm, 0.2 × 0.2 mm and 0.2 × 0.3 mm were studied. The performance results revealed that in most of the 10 models, the thrust was reduced for most J between 0.192 and 0.717. This implied that the presence of grooves

modified the flow characteristics only to detrimentally impact the thrust performance. However, the grooves improved power performance due to torque reduction. Analysis of K_P results showed in most of the 10 models the torque reduced compared to the baseline in the low to medium J operational range. The improvement in torque, however, did not contribute to improve η in all models. η is the critical parameter for operation of propellers in a UAV's real-flight.

REFERENCES

[1] A. Seeni, Effect of Groove Size on Aerodynamic Performance of a Low Reynolds Number UAV Propeller, *INCAS Bulletin*, vol. 14, no. 1, pp. 171–186, 2022, doi: 10.13111/2066-8201.2022.14.1.14.

[2] J. Brandt, R. Deters, G. Ananda, and M. Selig, Small-Scale Propeller Performance at Low Speeds – Online Database, 2010. http://www.ae.illinois.edu/m-selig/props/propDB.html (accessed May 01, 2018).